Secondary Relaxation in Metallic Glass Formers: Its Correlation with the Genuine Johari−Goldstein Relation

ARTICLE *in* THE JOURNAL OF PHYSICAL CHEMISTRY C · AUGUST 2009

Impact Factor: 4.77 · DOI: 10.1021/jp903777f

2 AUTHORS:

Lina Hu
Shandong University
28 PUBLICATIONS **368** CITATIONS
SEE PROFILE

Yuanzheng Yue
Aalborg University
209 PUBLICATIONS **2,721** CITATIONS
SEE PROFILE

Secondary Relaxation in Metallic Glass Formers: Its Correlation with the Genuine Johari−Goldstein Relaxation

Lina Hu*,† and Yuanzheng Yue†,‡

Key Laboratory of Liquid Structure and Heredity of Materials (Ministry of Education), Shandong University, Jinan 250061, China, and Section of Chemistry, Aalborg University, DK-9000 Aalborg, Denmark

Received: April 24, 2009; Revised Manuscript Received: July 7, 2009

We report experimental evidence for the existence of Johari−Goldstein (JG) relaxation in metallic glass formers. By using the hyperquenching−annealing−calorimetric approach, we study the dynamics of the secondary (β) relaxation in $La_{55}Al_{25}Ni_{20}$ metallic glasses. The observed β relaxation exhibits a typical feature of the genuine JG relaxation, i.e., the variation of its activation energy (E_β) with the glass transition temperature (T_g) obeys the relation $E_\beta = 26.8RT_g$. The correlative degree between the β and the primary α relaxations is closely associated with the liquid fragility. By a survey of the sub-T_g relaxation data of other metallic glass systems, we have determined the E_β values that find the correlation $E_\beta = 26.1RT_g$, indicating that JG relaxations are intrinsic in metallic glass formers. By analyzing the primitive relaxation time of the JG motion, $\tau_{0,JG}$, and the crossover time in the Coupling model, t_c, we discuss why the excess wing rather than the JG peak (or shoulder) is present in metallic glass systems.

1. Introduction

Although there is more than one type of secondary (β) relaxation preceding the primary (α) relaxation, it is now widely known that only the slow β relaxation plays an important role in the glass transition. In honor of Johari and Goldstein's discovery on rigid molecules in 1970s,[1,2] such slow β relaxations are commonly termed the Johari−Goldstein (JG) relaxations, which involve motion of all parts of a molecule rather than isolated motion of only a part of the molecules (such as the side groups).[3] Through a qualitative comparison between the relative strength of the JG peak in the dielectric spectrum and that of the α relaxation peak, it has been found that both relaxations have similar pressure and temperature dependences.[4,5] Besides, several common dynamic features have shown up in the JG relaxations in different materials such as polymers, ionic materials, and small molecules.[6] All the features of the JG relaxation reported in the literature indicate that the JG relaxation is the originator or precursor of the cooperative α relaxation and possesses the physical fundamentals.[7−9] All the features of JG relaxations are in accordance with each other in the coupling model (CM).[10]

Although progress has been made in the field of JG relaxations, some controversies still exist, e.g., about "heterogeneous" or "homogeneous"[11−14] and "the liquid-like region" or "the solid-like region".[6,12−14] Even the question of whether the JG relaxation is intrinsic or universal in glassy materials is not fully clarified, as well as the origin of the excess wing present on the high-frequency side of the α relaxation peak.[15,16] To solve these problems, many researchers have realized that metallic glasses, the β relaxations of which are rarely studied, are the potential candidates to study due to their particular dynamical properties.[17,18] For example, metallic glasses are regarded as systems with a dense packing of hard spheres, and the reorientation of the spheres around their axes does not contribute to that of the elastic dipole. These features could be used to clarify whether the translational motion of atoms contributes to the JG relaxation or only the reorientation of atoms does. By using isochronal mechanical spectroscopy, Pelletier et al. verified the existence of a β relaxation in $Pd_{43}Ni_{10}Cu_{27}P_{20}$ metallic glasses,[19] as later Hachenberg et al. did in $Pd_{77}Cu_6Si_{17}$.[20] JG relaxations were not reported in those works, and the β relaxation was roughly attributed to the existence of strong bonding of nonmetal−metal pairs in clustered units. The excess wing in mechanical relaxation curves was observed in $Zr_{65}Al_{7.5}Cu_{27.5}$ by Rösner et al.[17] and in $Zr_{46.75}Ti_{8.25}Cu_{7.5}Ni_{10}Be_{27.5}$ and $Ce_{70}Al_{10}Cu_{20}$ by Wang et al.[18,21] These studies speculated that the excess wing found in amorphous alloys was due to the hidden JG relaxation, but they did not detect the dynamic characteristics of the β relaxation reflected by the excess wing. As emphasized by Ngai et al.,[6] the identification of β relaxations with JG relaxations should proceed with caution. With this in mind, an effort was once made to compare the results predicted from the coupling model with the experimental results of the excess wing.[22] The experimental verification based on detecting dynamic features of the β relaxation, however, is still lacking in metallic glass formers.

It is noted that the dielectric spectroscopy often used elsewhere (such as in polymers) is not suitable for metallic glasses, due to the high conductivity of the materials. Dynamical mechanical relaxation experiments are also not applicable to investigating β relaxations in metallic glasses, since only the excess wing is observed, as depicted in many strong glass formers. In order to probe into β relaxations in metallic glasses, the hyperquenching−annealing−calorimetric scan (HAC) approach is applied in the present work, where the rationale is to first slow down the motions with higher frequency than the frequency range involved in the α relaxation, and then see what happens to the higher-frequency relaxation behavior in the β frequency range.[23] By using the HAC, the present work studies the enthalpy relaxation dynamics of the hyperquenched (HQ)

* Corresponding author. Tel: 0086-531-88395011; Fax: 0086-531-88395011, E-mail: hulina0850@mail.sdu.edu.cn.
† Shandong University.
‡ Aalborg University.

10.1021/jp903777f CCC: $40.75
Published on Web 07/24/2009

$La_{55}Al_{25}Ni_{20}$ glass well below T_g, and then discusses the data in terms of the sub-T_g relaxation of other HQ metallic glasses.

2. Experimental Methods

$La_{55}Al_{25}Ni_{20}$ master alloys were prepared by melting the elemental metals with purities ranging 99.9−99.999% in an arc furnace under argon atmosphere. The hyperquenching of the master alloys was realized by the single copper roller melt-spinning technique in high-purity argon atmosphere. The master alloys were remelted by using the high-frequency induction and rapidly solidified into continuous ribbons at the circumferential velocity of 40 m/s. The ribbons are about 50−70 μm in thickness and 4−6 mm in width. According to the method introduced previously,[24] the cooling rate of the hyperquenched ribbons was about 10^6 K/s.

The HQ $La_{55}Al_{25}Ni_{20}$ ribbons were annealed in a furnace under argon atmosphere at selected temperatures (T_a) well below T_g (493 K) for various durations. The error range of T_a is ±1 K. The isobaric heat capacity (C_p) of the samples was measured using a differential scanning calorimeter (DSC) (Netzsch DSC404) in the nitrogen with a flow rate of 30 cm^3/min. The sensitivity and temperature were calibrated using the standard procedure reported elsewhere.[25] The sample mass was approximately 20 mg. The samples were placed in a platinum crucible situated on a sample holder of the DSC at room temperature. The samples were held 5 min at an initial temperature of 303 K, and then heated at a "standard" rate of 20 K/min to 543 K, and then cooled back at 20 K/min to 343 K; thus, the so-called standard glass is obtained. After natural cooling to room temperature, the second upscan was performed on the standard glass using the same procedure as used in the first upscan. To determine the heat capacity (C_p) of the samples, both the baseline (blank) and the reference sample (sapphire) were measured. The glass transition temperature (T_g) was determined as the onset temperature of the glass transition peak on the second upscan C_p curve, i.e., the temperature of the intersection between the extrapolated line of the glass C_p and the extrapolated line of the rapidly rising C_p.

Our previous work[23] has shown that the HAC approach not only allows the detection of the total enthalpy change below T_g, but also gives a detailed pattern of the enthalpy relaxation, as well as the average time of β relaxations, τ_β. Figure 1 shows the C_p curve of the partially annealed ribbons, i.e., the first upscan curve (C_{p1}), and the C_p curve of the standard sample, i.e., the second upscan curve (C_{p2}), respectively. The curve C_{p2} is termed the "standard curve". The area between C_{p1} and C_{p2} represents the unrelaxed or remaining part of the excess enthalpy of the HQ glasses annealed for a duration t relative to that of the standard glass, $\Delta H_{remain}(t)$. Normalizing $\Delta H_{remain}(t)$ by ΔH_{total} ($\Delta H_{remain}(t = 0)$) leads to the relaxation function $\phi(t)$:

$$\frac{\Delta H_{remain}(t)}{\Delta H_{total}} = \phi(t) \quad (1)$$

which can be described by the Kohlrausch function

$$\phi(t) = \exp\left[-\left(\frac{t}{\tau_\beta}\right)^{1-n}\right] \quad (2)$$

where t is the annealing time and $(1 - n)$ is the stretching exponent. The average relaxation time τ_β and the value $(1 - n)$ were obtained by fitting the Kohlrausch function (eq 2) to the $H_{remain}(t)/\Delta H_{total}$ data.

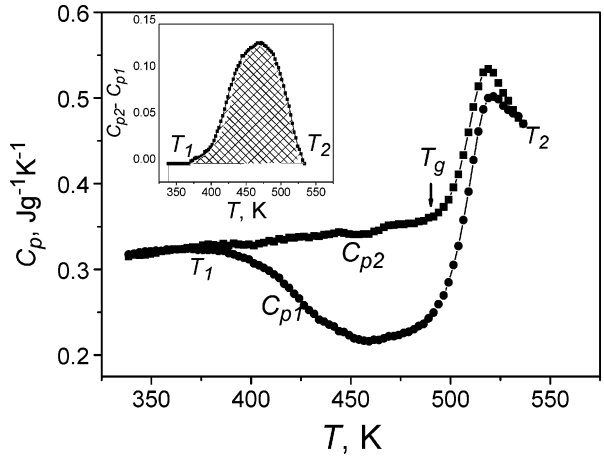

Figure 1. Heat capacity curves of hyperquenched $La_{55}Al_{25}Ni_{20}$ ribbons annealed for a duration t ($T_a = 373$ K, $t = 30$ min). C_{p1} and C_{p2} represent the heat capacity curves measured during the first and second upscans of the DSC measurements, respectively. T_1 is the onset temperature, at which the release of enthalpy starts, and T_2 is the temperature at which $C_{p1} = C_{p2}$. The inset shows the changes of the excessive heat capacity ($C_{p2} - C_{p1}$) as a function of temperature. The hatched area corresponds to the remaining excess enthalpy of HQ glasses after annealing relative to that of standard glasses, $\Delta H_{remain}(t)$: $\Delta H_{remain}(t) = \int_{T_1}^{T_2}(C_{p2} - C_{p1})\,dT$.

3. Results and Discussion

3.1. Enthalpy Relaxation Dynamics of the Hyperquenched (HQ) $La_{55}Al_{25}Ni_{20}$ Glass Ribbons Well Below T_g. Figure 2a shows a set of representative C_p measurements on the HQ $La_{55}Al_{25}Ni_{20}$ glass ribbons annealed at different temperatures for a constant duration. For a comparison, the experimental C_p curves of HQ $(Fe_{0.5}Ni_{0.5})_{83}P_{17}$ ribbons are shown in Figure 2b.[26] In Figure 2a, the curves A−G exhibit distinct exothermic peaks. The area enclosed by the C_{p2} and C_{p1} curves as shown in Figure 1 decreases with increasing annealing temperature, T_a, indicating that the trapped excess enthalpy is released during annealing procedure and the structural configuration approaches a lower energy level. This tendency of energy recovery with T_a is also observed in Figure 2b. It is noted that in Figure 2b each C_p curve shows two endothermic peaks, while in Figure 2a, only the second endothermic peak, i.e., the glass transition peak, is present. The first endothermic peak, which occurs prior to the exothermic peak (i.e., the energy release peak), has been referred to as a "sub-T_g peak" or a "shadow T_g peak" or a prepeak.[27] The presence of the sub-T_g peak means that during annealing some microregions with fast relaxation reach the lower energy states relative to the rest of glass and then return to the higher energy states during DSC upscan. It is noted that $La_{55}Al_{25}Ni_{20}$ metallic glasses, for which the fragility parameter m equals 32, are stronger than other metallic systems, where the m values range from 35 for $Zr_{65}Al_{7.5}Cu_{27.5}$ to 331 for $Al_{84}Ni_{10}La_3Ce_3$.[28,29] Not only in Fe-based alloys,[26] but also in other fragile metallic systems (such as Zr-, Al-, Pd-),[30−32] distinct sub-T_g peaks have been reported. This indicates that fragile metallic glass formers exhibit distinct sub-T_g peaks in calorimetric scans. The dependence of the sub-T_g peak intensity on the fragility is also observed in the oxide glass formers[33,34] if we compare Figure 2c with Figure 2d: The typical strong glass GeO_2 lack the sub-T_g peak, while the sub-T_g peak is quite distinct in the fragile basaltic glass. The presence of the sub-T_g peak suggests more

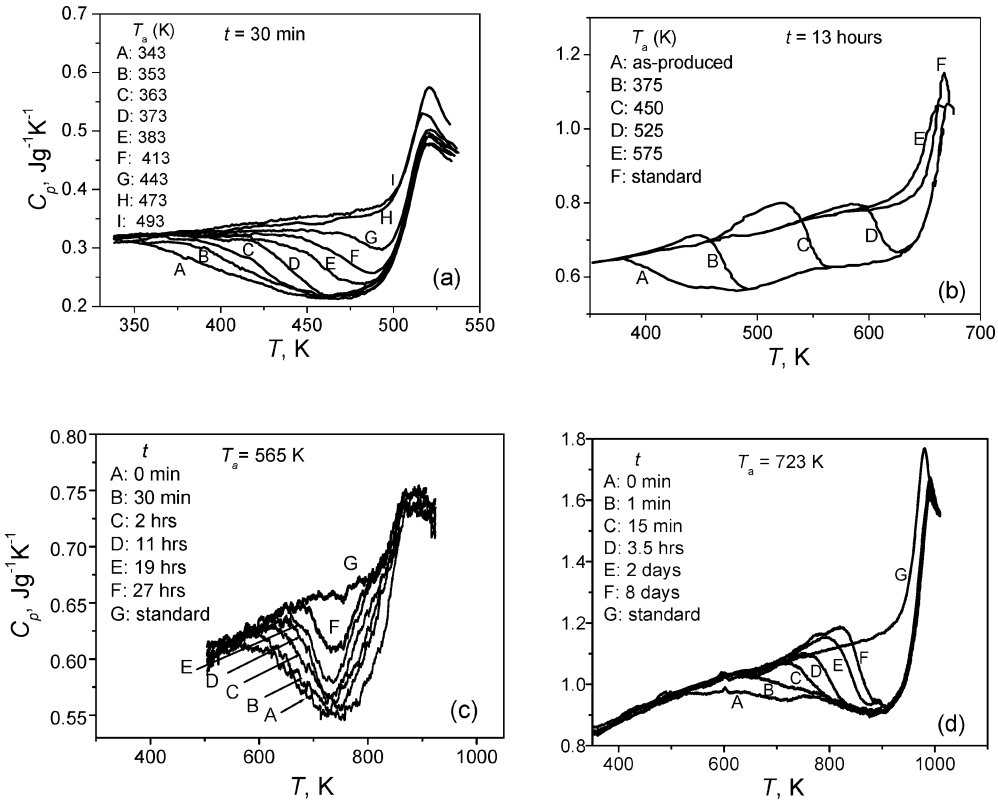

Figure 2. Influence of annealing procedure on the energy release of hyperquenched glasses: (a) $La_{55}Al_{25}Ni_{20}$ annealed at different temperatures T_a for $t_a = 30$ min; (b) $(Fe_{0.5}Ni_{0.5})_{83}P_{17}$ annealed at different temperatures for 13 h;[26] (c) GeO_2 annealed at $T_a = 565$ K for different durations;[23] (d) basaltic fibers annealed at $T_a = 723$ K for different durations.[24]

structural heterogeneity in fragile glass formers than that in strong glasses.

Besides the influence of fragility on the intensity of the sub-T_g peak, the influence of annealing temperature (or annealing time) on the shape of the C_p curves is worth noting. In Figure 2a, when the annealing is performed below 413 K (curves A−E), the glass transition is not affected, indicated by the overlap of the C_p curves above T_g for both the annealed and unannealed ribbons. This indicates that the low-temperature annealing does not influence the slow, cooperative α relaxation, but affects the β relaxation in high-frequency regions. In contrast, at $T_a > 413$ K (curves G−I), not only do the C_p curves below T_g change toward the standard curve, but also the overlapping degree of the C_p curves above T_g gradually decreases with increasing T_a. This indicates that both the α relaxation and the β relaxation are affected. In an earlier work, it was suggested that, for strong glass formers, every relaxation unit involved in β relaxations contributes to the primary relaxation process, i.e., "no β without α" picture proposed by Donth et al.[35] However, it is easier to separate the slow α cooperative motion from the local β relaxation in fragile glasses. This view is verified by Figure 2. In accordance with the fact that the fragility of the HQ $La_{55}Al_{25}Ni_{20}$ ribbons is between the fragilities of GeO_2 (m = 18) and basaltic glasses (m = 62.4), Figure 2a seems to transform from Figure 2d into Figure 2c with increasing T_a: For basaltic glasses in Figure 2d, increasing the annealing time tends to only influence the shape of the C_p curve below T_g, but leaving the C_p curve above T_g unaffected. For HQ GeO_2 fibers in Figure 2c, however, the change of shape of the C_p curve below T_g is always accompanied with that above T_g. We notice that this influence of the fragility strength on the correlation between the β and the α relaxations could be explained intuitively by the theoretical framework of the potential energy

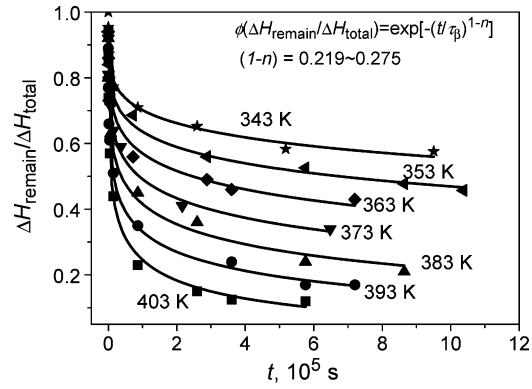

Figure 3. Annealing duration (t) dependence of the normalized remaining excess enthalpy (H_{remain}/H_{total}) in the HQ $La_{55}Al_{25}Ni_{20}$ glass ribbons annealed at different temperatures below 413K. The solid lines are the fits of eq 2.

landscape (PEL).[36] It has been reported[37] that the density of the energy minimum for an N-atom system for metallic glass formers ranges from exp(1.6N) to exp(3.0N), which is larger than ~exp(1.2N) of a GeO_2 glass with typical network structures, and is much smaller than those of fragile materials with different atomic packing. Fewer megabasins in less fragile glasses lead to the larger degree of the overlap between the α and β relaxations.

Figure 3 shows the time dependence of the normalized remaining excess enthalpy in the HQ $La_{55}Al_{25}Ni_{20}$ glass ribbons annealed at different temperatures below 413 K. The H_{total} in the fresh HQ ribbons is in the range 13−15 J/g, and the relaxation behavior described by the Kohlrausch function (eq 2) is found for each annealing temperature, as depicted by the solid lines in Figure 3. It is found that the average relaxation time τ_β decreases with increasing temperature as expected,

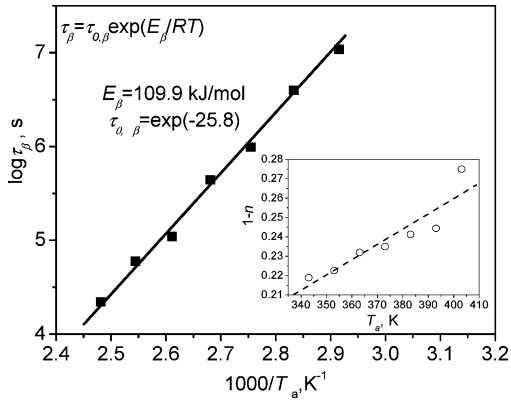

Figure 4. Dependence of the characteristic relaxation time (τ_β) of the secondary relaxation on the reciprocal annealing temperature ($1/T_a$). Inset: the plot of the stretching exponent ($1 - n$) against T_a. The dashed line is only a guide for eyes.

accompanied by a slight increase in ($1 - n$) within the limit error. According to Figure 3, the average relaxation time of τ_β is plotted in Figure 4 as a function of the inverse annealing temperature T_a. It is observed that the $\log\tau_\beta \sim T_a^{-1}$ relationship obeys the Arrhenius equation (correlation coefficient 0.987) with the activation energy, E_β, of 109.9 ± 8 kJ/mol. Here, it should be pointed out that at low T_a there is a large uncertainty of the τ_β value, due to the limited data points for each T_a and only partial enthalpy decay. For example, at 343 K the error of τ_β is ±17.9%, and it is reduced with increasing T_a. The relationship of $\log\tau_\beta \sim T_a^{-1}$, however, depends strongly on the order of magnitude of τ_β, especially at low temperatures where the τ_β is quite large. It leads to the small error of the E_β value in the Arrhenius equation in Figure 4, compared with that of the τ_β values in Figure 3. The temperature dependence of the ($1 - n$) derived from Figure 3 is shown in the inset of Figure 4. These calculated ($1 - n$) values are in accordance with the relationship observed between the fragility parameter m and the relaxation time dispersion α_{cc} of β dielectric relaxations, e.g., a small m corresponds to a small α_{cc}.[38]

According to Figure 4, the E_β value for the β relaxation of $La_{55}Al_{25}Ni_{20}$ glasses equals to $26.8RT_g$. This $E_\beta \sim T_g$ relationship is close to the empirical relation of JG relaxations found in polymers, small molecules, and ionic liquids.[9,39] For non-JG β relaxations, the values of E_β/RT_g are around 13, much less than 20.[40,41]

3.2. Dynamics of Sub-T_g Enthalpy Relaxation of Other Metallic Glass Systems. More than 20 years ago, systematic studies of enthalpy relaxation behavior were carried out on a number of HQ metal−metalloid and metal−metal ribbons by other researchers.[26,30−32,42] For instance, by observing the annealing temperature T_a dependence of the maximum differential specific heat difference, $\Delta C_{p,max}$, it has been found that the enthalpy relaxation of PdNiP, (Fe, Ni)-P, ZrCuNiAl, AlNiCe alloys upon annealing occurs by two separable stages with different mechanisms.[42] The first-stage relaxation (called "sub-T_g" relaxation in the present work) was attributed to the local-range or medium-range atomic rearrangements with high frequency relative to that of the α process responsible for the second stage near (or slightly below) T_g. This finding is in accordance with the recent work, which reports that at low annealing temperatures the activation energy of the initial relaxation stage tends to approach that of the β or JG relaxation.[43] In this context, we attempt to reanalyze the previous experimental data of metallic glasses in order to see whether the β relaxations reflected by the first-stage relaxation are correlated to JG motions.

TABLE 1: Activation Energy E_β of Sub-T_g Relaxations, Glass Transition Temperature T_g, and Temperature T' Where the Maximum Differential Specific Heat Difference $\Delta C_{p,max}$ Is Present in Metallic Glasses

metallic glasses	E_β, kJ/mol	T_g, K	T', K	E_β/RT_g	ref no
$(Fe_{0.85}Ni_{0.15})_{83}P_{17}$	134	650	475	24.8	42
$(Fe_{0.85}Cr_{0.15})_{83}P_{17}$	150	720	525	25.1	42
$(Fe_{0.85}V_{0.15})_{83}P_{17}$	162	728	600	26.8	42
$(Fe_{0.85}Mo_{0.15})_{83}P_{17}$	189	754	575	30.1	42
$(Fe_{0.75}Ni_{0.25})_{83}P_{17}$	111	640	450	20.8	42
$(Fe_{0.75}Co_{0.25})_{83}P_{17}$	146	685	500	25.6	42
$(Fe_{0.75}Mn_{0.25})_{83}P_{17}$	141	697	500	24.3	42
$(Fe_{0.75}Cr_{0.25})_{83}P_{17}$	166	765	550	26.1	42
$(Fe_{0.5}Ni_{0.5})_{83}B_{17}$	172	650	525	31.9	26
$(Fe_{0.5}Ni_{0.5})_{83}P_{17}$	154	645	450	28.7	26
$Pd_{48}Ni_{32}P_{20}$	92.4	582	460	19.1	31
$Al_{82}Ni_{10}Ce_8$	158	585	425	32.0	32
$Pd_{43}Ni_{10}Cu_{27}P_{20}$[a]	105.9	568	473	22.4	19
$Pd_{40}Ni_{10}Cu_{30}P_{20}$[a]	128.9	575	397	26.9	44
$Zr_{46.75}Ti_{8.25}Cu_{7.5}Ni_{10}Be_{27.5}$[a]	138.4	628	478	26.5	44
$Zr_{65}Cu_{15}Ni_{10}Al_{10}$[a]	130.8	654	491	24.0	44
$(Cu_{50}Zr_{50})_{92}Al_8$[a]	174.1	692	505	30.2	44, 45
$La_{57.5}(Cu_{50}Ni_{50})_{25}Al_{17.5}$[a]	92.4	435	308	25.5	44

[a] T' was determined at the testing frequency of 1 Hz in dynamic mechanical experiments.

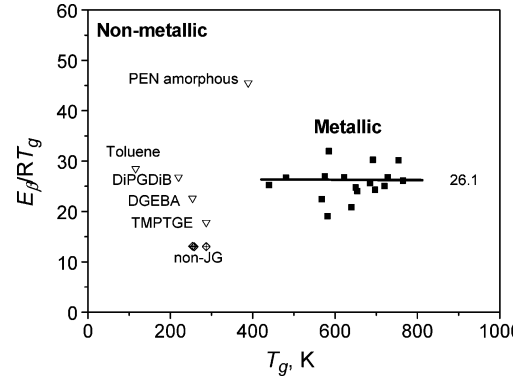

Figure 5. The values of E_β/RT_g for different types of materials. The metallic glasses correspond to those shown in Table 1, as well as $La_{55}Al_{25}Ni_{20}$ in the present work. The examples of nonmetallic glasses are taken from ref 9. The solid line represents the average value of E_β/RT_g for metallic glass formers.

Table 1 shows compilations of the sub-T_g relaxation data in different metallic glass systems. The β relaxation data derived from dynamical mechanical analysis are also listed in the table.[19,44] It is found that all T' values, where $\Delta C_{p,max}$ presents metallic glasses values, are well below T_g ($T' \leq T_g - 100$ K), indicating that the temperature range where the β relaxations can be detected is quite similar to that of JG relaxations commonly seen in polymers and molecular glasses.[6] In order to exclude the influence of the α relaxation on the changes of $\Delta C_{p,max}$, only the protocols for the annealing temperatures T_a below or around T' are considered in this work.

As shown in Table 1, E_β/RT_g ranges from 19.1 to 32 for metallic glass formers for both DSC and DMA methods. The average value E_β/RT_g for these metallic glass formers is 26.1. This value agrees with the ratios between the JG activation energy E_{JG} and T_g for polymers, small molecules, and ionic liquids.[9] In order to further demonstrate the relationship between β relaxations (Table 1) with genuine JG relaxations, Figure 5 is plotted, where the E_β/RT_g values between different types of glass formers are compared. The striking difference is that the

scattering range of the E_β/RT_g values for metallic glass formers is evidently less than that for the nonmetallic glass formers (from 15.6 for 2-ethyl-1-hexanol to 45.5 for amorphous PEN).[9] This phenomenon agrees with the difference in the data scattering range of the nonexponential parameter $(1 - n)$ of primary relaxations between metallic and nonmetallic liquids. The $(1 - n)$ values of the former are centered around 0.5,[46] whereas those of the latter are from 0.3 to 0.75.[38] The molecular dynamics simulation studies indicate that the relatively small scattering of the parameter $(1 - n)$ of the metallic glass formers is due to their hard sphere structure with dense packing.[47,48] In terms of the coupling model, the close relationship between E_β/RT_g and $(1 - n)$ has been described by the equation[9]

$$E_\beta/RT_g = 2.303[(1 - n)\log_{10}\tau_\alpha(T_g) + n\log_{10}t_c - \log_{10}\tau_{0,\beta}] \quad (3)$$

where t_c is the temperature-insensitive crossover time, determined by the strength of the intermolecular interaction. For small molecular and polymeric glass formers, t_c of 2 ps is usually adopted.[7−10] For metallic glasses, however, t_c should be much larger than 2 ps. The success of the cluster kinetics model in metallic glass formers[49] indicates that the potential energy of the clusters should be incorporated in eq 3, rather than the potential energy between molecules considered in molecular liquids. This scenario is supported by the comparisons in the value of the primitive relaxation time of β relaxation, $\tau_{0,\beta}$, between metallic glass formers and nonmetallic glass formers. In any circumstance, t_c should be longer than $\tau_{0,\beta}$. The $\tau_{0,\beta}$ values for small molecular and polymeric glass formers are $10^{-13}-10^{-18}$ s, while those of amorphous $(Fe-M)_{83}P_{17}$ (M = V, Cr, Mo, Mn, Co, Ni) alloys are 10^{-9} to 10^{-12} s.[42] A large t_c value corresponds to a large τ_{JG} (T_g) value according to the following expression:[6,7]

$$\log_{10}\tau_{JG}(T_g) = n\log_{10}t_c + (1 - n)\log_{10}\tau_\alpha(T_g) \quad (4)$$

where $\tau_\alpha(T_g)$ is around 100 s. It maybe explains why metallic glasses generally display the excess wing, rather than JG relaxation peaks in dynamical mechanical experiments.

The discussions above reveal that the β relaxations in metallic glass formers bear the typical feature of genuine JG relaxation, i.e., a typical $E_\beta \sim T_g$ relation for JG type. Besides, three other characteristics of JG relaxations are also observed in metallic glasses.[26,30−32,42] First, the sub-T_g relaxation has an Arrhenius temperature dependence of τ_β. Second, for $(Fe-M)_{83}P_{17}$(M = V, Cr, Mo, Mn, Co, Ni) amorphous ribbons (In Table 1), the decrease in the group number of M metals shifts the distribution of the sub-T_g relaxation entity to a higher temperature range, and decreases the magnitude of the relaxation entity. These tendencies are in accordance with what has been observed in dielectric spectrum experiments in many polymers and small molecules, i.e., the smaller the separation between the α and the JG relaxation peaks is, the weaker the relative strength of the JG relaxation peak.[6] Third, the intensity of the sub-T_g relaxation spectrum (i.e., the first-stage relaxation) relative to the total spectrum decreases with decreasing quenching rates. On the basis of all of these observations, it is reasonable to identify the β relaxations in Table 1 as the genuine JG relaxations. This offers important evidence for the universality of the JG relaxation in glassy materials.

4. Conclusions

A close relationship has been observed in metallic glasses between liquid fragility and the intensity of the sub-T_g peak, as well as that between liquid fragility and the correlative degree between the β and α relaxations. In different systems of metallic glass formers, the typical feature of JG relaxations concerning the relation between the activation energy and T_g has been identified. This verifies the generality and the intrinsic nature of JG relaxations in glassy materials. Since amorphous metallic alloys (neither intramolecular nor rotational degrees of freedom) are different from polymeric and molecular materials, the present work casts light on probing into the common features of JG relaxations, as well as their particularity in different materials. Because of the large crossover time t_c in metallic glass systems, we believe that the potential energy of clusters involved in JG relaxations is a dominant factor in metallic glasses that we should pay attention to in the next work.

Acknowledgment. We thank K. L. Ngai for valuable discussions. This work was supported by National Basic Research Program of China (grant no. 2007CB613901), National Natural Science Foundation of China (grant no. 50801041 and 50871061), and Research Fund for the Doctoral Program of Higher Education of China (grant no. 200804221041).

References and Notes

(1) Johari, G. P.; Goldstein, M. *J. Chem. Phys.* **1970**, *53*, 2372.
(2) Johari, G. P.; Goldstein, M. *J. Chem. Phys.* **1972**, *55*, 4245.
(3) (a) McCrum, N. G.; Read, B. E.; Williams, G. *Anelastic and Dielectric Effects in Polymeric Solids*; Wiley: London, 1967. (b) Boyer, R. F. *Polymer* **1976**, *17*, 996.
(4) (a) Hensel-Bielowka, S.; Paluch, M.; Ziolo, J.; Roland, C. M. *J. Phys. Chem. B* **2002**, *106*, 12459. (b) Köplinger, J.; Kasper, G.; Hunklinger, S. *J. Chem. Phys.* **2001**, *113*, 4701.
(5) Kudlik, A.; Tschirwitz, C.; Benkhof, S.; Blochowicz, T.; Rössler, E. *Europhys. Lett.* **1997**, *40*, 649.
(6) Ngai, K. L.; Paluch, M. *J. Chem. Phys.* **2004**, *120*, 857.
(7) Ngai, K. L. *J. Chem. Phys.* **1998**, *109*, 6982.
(8) Ngai, K. L. *Phys. Rev. E* **1998**, *57*, 7346.
(9) Ngai, K. L.; Capaccioli, S. *Phys. Rev. E* **2004**, *69*, 031501.
(10) Ngai, K. L.; Capaccioli, S. *J. Phys.: Condens. Matter.* **2007**, *19*, 205114.
(11) Williams, G.; Watts, D. C. *Trans. Faraday Soc.* **1971**, *67*, 1971.
(12) Johari, G. P. *J. Non-Cryst. Solids* **2002**, *317*, 307–310.
(13) Johari, G. P. *Plastic deformation of amorphous and semi-crystalline materials*; Les Edition de Physique: Les Ullis, 1983.
(14) Tanaka, H. *J. Non-Cryst. Solids* **2005**, *351*, 3396.
(15) (a) Dixon, P. K.; Wu, L.; Nagel, S. R.; Williams, B. D.; Carini, J. P. *Phys. Rev. Lett.* **1990**, *65*, 1108. (b) Leheny, R. L.; Nagel, S. R. *Europhys. Lett.* **1997**, *39*, 447.
(16) Lunkenheimer, P.; Loidl, A. *Chem. Phys.* **2002**, *284*, 205.
(17) Rösner, P.; Samwer, K.; Lunkenheimer, P. *Euro. Phys. Lett.* **2004**, *68*, 226.
(18) Liu, X. F.; Zhang, B.; Wen, P.; Wang, W. H. *J. Non-Cryst. Solids* **2006**, *352*, 4013.
(19) Pelletier, J. M.; Van de Moortèle, B.; Lu, I. R. *Mater. Sci. Eng. A* **2002**, *336*, 190.
(20) Hachenberg, J.; Samwer, K. *J. Non-Cryst. Solids* **2006**, *352*, 5110.
(21) Wen, P.; Zhao, D. Q.; Pan, M. X.; Wang, W. H.; Huang, Y. P.; Guo, M. L. *J. Appl. Phys.* **2004**, *84*, 2790.
(22) Ngai, K. L. *J. Non-Cryst. Solids* **2006**, *352*, 404.
(23) Hu, L. N.; Yue, Y. Z. *J. Phys. Chem. B* **2008**, *112*, 9053.
(24) (a) Yue, Y. Z.; von der Ohe, R.; Jensen, S. L. *J. Chem. Phys.* **2004**, *120*, 8053. (b) Yue, Y. Z.; Jensen, S. L.; Christiansen, J. D. *Appl. Phys. Lett.* **2002**, *81*, 2983.
(25) Sarge, S. M.; Gmelin, E.; Höhne, G. W. H.; Cammenga, H. K.; Hemminger, W.; Eysel, W. *Thermochim. Acta* **1994**, *247*, 129.
(26) Chen, H. S.; Inoue, A.; Masumoto, T. *J. Mater. Sci.* **1985**, *20*, 2417.
(27) (a) Yue, Y. Z.; Angell, C. A. *Nature* **2004**, *427*, 717. (b) Johari, G. P. *J. Chem. Phys.* **2003**, *119*, 2935.
(28) Perena, D. N. *J. Phys.: Condens. Matter.* **1999**, *11*, 3807.
(29) Novikov, V. N.; Sokolov, A. P. *Phys. Rev. B* **2006**, *74*, 064203.
(30) Inoue, A.; Masumoto, T.; Chen, H. S. *J. Mater. Sci.* **1985**, *20*, 4057.
(31) Chen, H. S.; Coleman, E. *Appl. Phys. Lett.* **1976**, *28*, 245.

(32) Kim, Y. H.; Inoue, A.; Masumoto, T. *J. Non-Cryst. Solids* **1991**, *127*, 233.
(33) (a) Hodge, I. M. *Macromolecules* **1983**, *16*, 898. (b) Pappin, A. J.; Hutchinson, J. M.; Ingram, M. D. *Macromolecules* **1992**, *25*, 1084.
(34) Berens, A. R.; Hodge, I. M. *Macromolecules* **1982**, *15*, 756.
(35) Donth, E. *The glass transition: relaxation dynamics in liquids and disordered materials*; Springer: Berlin, 2001.
(36) (a) Stillinger, F. H. *Science* **1995**, *267*, 1935. (b) Angell, C. A. *Nature* **2001**, *410*, 261.
(37) Hu, L. N.; Bian, X. F.; Wang, W. M.; Liu, G. R.; Jia, Y. B. *J. Phys. Chem. B* **2005**, *109*, 13737.
(38) Wang, L. M.; Richert, R. *Phys. Rev. B* **2007**, *76*, 064201.
(39) Rivera, A.; Rössler, E. A. *Phys. Rev. B* **2006**, *73*, 212201.
(40) Pisignano, D.; Capaccioli, S.; Casalini, R.; Lucchesi, M.; Rolla, P. A.; Justl, A.; Rössler, E. *J. Phys.: Condens. Matter.* **2001**, *13*, 4405.
(41) Corezzi, S.; Beiner, M.; Huth, H.; Schröter, K.; Capaccioli, S.; Casalini, R.; Fioretto, D.; Donth, E. *J. Chem. Phys.* **2002**, *117*, 2435.
(42) Inoue, A.; Masumoto, T.; Chen, H. S. *J. Non-Cryst. Solids* **1986**, *83*, 297.
(43) Chen, K.; Vyazovkin, S. *J. Phys. Chem. B* **2009**, *113*, 4631.
(44) Zhao, Z. F.; Wen, P.; Shek, C. H.; Wang, W. H. *Phys. Rev. B* **2007**, *75*, 174201.
(45) Cheung, T. L. Thesis (M. Phil.): Mechanical and surface properties of copper-based bulk metallic glasses; City University of Hongkong, Hongkong, 2006.
(46) Wang, L. M.; Liu, R. P.; Wang, W. H. *J. Chem. Phys.* **2008**, *128*, 164503.
(47) (a) Scopigno, T.; Ruocco, G.; Sette, F. *Rev. Mod Phys.* **2005**, *77*, 881. (b) Moreno, A. J.; Colmenero, J. *J. Chem. Phys.* **2006**, *125*, 164507.
(48) (a) Foffi, G.; Götze, W.; Sciortino, F.; Tartaglia, P.; Voigtmann, Th. *Phys. Rev. Lett.* **2003**, *91*, 085701. (b) Foffi, G.; Götze, W.; Sciortino, F.; Tartaglia, P.; Voigtmann, Th. *Phys. Rev. E* **2004**, *69*, 011505.
(49) Hu, L. N.; Bian, X. F.; Wang, W. M.; Zhang, J. Y.; Jia, Y. B. *Acta Mater.* **2004**, *52*, 4773.
(50) Inoue, A.; Zhang, T.; Masumoto, T. *J. Non-Cryst. Solids* **1992**, *150*, 396.

JP903777F